Switchable Structures using Asymmetric Composite Laminates – Two Case Studies

Vishrut Deshpande[a], Oliver Myers[a], and Suyi Li[a]

[a]Department of Mechanical Engineering, Clemson University, Clemson, SC

ABSTRACT

Asymmetric carbon fiber reinforced composites have shown immense potentials in adaptive structure applications such as morphing airfoils,[1–4] and energy harvesters.[5] Due to the unidirectional prepregs used for their fabrication and strongly nonlinear behaviors, these composite laminates can show significantly different load-displacement responses along with different loading directions. Moreover, asymmetric composites can exhibit bistability, offering a pathway to easily switch between different mechanical responses. This paper presents two switchable structure concepts based on asymmetric composites. The first concept exploits two distinct responses in the [0°/90°] laminates in two perpendicular in-plane directions. Via a simple snap-through, such structure can switch between stiff and compliant. Preliminary experiments show that it can achieve close to 70:1 stiffness ratio between these two configurations. The second concept is a Kresling origami structure fabricated in a novel way using asymmetric fiber composites and 3D-printed flexible TPU material. Due to the asymmetric layup in their triangular composite facets, the Kresling structure can switch from a "foldable" configuration to a "locked" configuration. Axial compression and tension response for foldable and locked configurations are experimentally investigated. These two case studies suggest that there are still many untapped potentials in the asymmetric fiber composites for advanced and multi-functional structural applications.

Keywords: Asymmetric laminates; Variable Stiffness, Kresling, Locking

1. INTRODUCTION

Asymmetric carbon fiber reinforced composites have gained significant interest in the past two decades due to their lightweight, simplistic design, and most importantly, bi-stability: a unique phenomenon that the composite can settle into two different stable configurations without external aids. Such bistability originates from the internal residual stress developed during curing due to its asymmetric ply layup. Here, asymmetric layup usually refers to a non-symmetrical distribution of ply configuration about its mid-plane, such as a simple [90°] layer over a [0°] layer: [90°/0°] laminate. A bistable asymmetric composite can be easily switched from one stable state to the other through external stimuli; this process is often called snap-through. There have been rigorous studies done in order to understand how the geometrical parameters of asymmetric composites — such as ply orientations, initial shape, and ply thickness — influence their overall performance.[6–9] Based on the results of these fundamental studies, asymmetric composite has found applications in many fields such as renewable energy harvesting structures,[9–12] morphing airframes,[1,3,4,13] and adaptive automobile structures.[14]

Due to the use of unidirectional carbon fiber reinforced polymers (CFRP) prepregs for fabrication, the mechanical properties of asymmetric composite laminates become highly dependent on loading directions.[7,15–17] It is well understood that stimuli (e.g., mechanical displacement or force) in the transverse, out-of-plane direction to the laminate could serve as a snap-through load, generating shape change from one stable shape to the other. Many researches have relied on such out-of-plane transverse loading to understand the laminates' deformation characteristics,[15,16,18] predicting the deformation behaviours through analytical or simulation approach,[6,9,17] and exploring different actuation methods.[19–22] However, in-plane loading of asymmetric composites generates far different responses than the out-of-plane loading. For example, Arrieta et al., in their studies, showed two drastically different responses from a multi-patched laminate strip under in-plane loading – a curved shape that

Further author information: (Send correspondence to Vishrut Deshpande)
E-mail: vdeshpa@clemson.edu

Active and Passive Smart Structures and Integrated Systems XVI, edited by Jae-Hung Han
Shima Shahab, Jinkyu Yang, Proc. of SPIE Vol. 12043, 120430H
 · 0277-786X · doi: 10.1117/12.2612988

provides a soft/deformable response and a straight shape that provides a stiffer response.[7] This multi-patched laminate strip is flattened out at the edges to enhance its embeddability to a morphing wing structure.[4]

Nonetheless, far-less attention has been dedicated to the in-plane loading response of asymmetric composites despite the promising application potentials. More importantly, innovatively integrating and loading the asymmetric laminates can foster new multi-functional structural systems that can switch between fundamentally different behaviors. To this end, this study exploits the in-plane loading behaviors of asymmetric CFRP laminates to achieve *switchable* performance in two different structures — one switching between two different stiffness modes and the other switches between two different deformation (or morphing) modes.

The first example is a sandwich structure consisting of three asymmetric laminates stacked parallel and assembled with two end plates. A simple snap-through process can switch the curvature of the load-bearing laminates. As a result, this sandwich structure can switch between stiff and compliant configurations.

The second example is a deployable structure inspired by the *Kresling* origami pattern. By integrating asymmetric laminates into the Kresling's facets, we introduce a locking feature through the help of bistability: The Kresling facets can buckle outwards, resisting any change to its shape. As a result, the Kresling can switch between a foldable configuration and a locked configuration with significantly higher load-bearing capacity.

High strength-to-weight ratio, directional stiffness, and reliable bistability[23] of asymmetric laminates can advance the field of adaptive structures that are lightweight, rapidly manufactured, and easy to use. The switchable modes introduced by the new structures – one allowing the stiffness switching, and the other morphing capability switches – can add new functionalities to the asymmetric composites. Moreover, the switching between the two modes is a product of the bistability nature of these laminates, so no external aids are required to maintain their switched state. Hence, the results of this study open new avenues towards exploiting the potential of bistable CFRPs to advance and enrich the functionalities of adaptive structural systems for many different applications.

2. CASE STUDY 1: SWITCHABLE DUAL-STIFFNESS SANDWICH STRUCTURE

By a simple construction, we assemble asymmetric and bistable CFRP laminates to create a sandwich structure. This structure features two endplates that provide the basis for testing the overall compression responses in two distant configurations – "stiff" configuration and "compliant" configuration (Figure 1). The sandwich structure provides a significant stiffness variation by a simple snap-through process. In this case study, we discuss the construction of the proposed sandwich structure, finite simulation for determining the optimal connection between composite laminate and endplates, and proof-of-concept experiments showcasing both stiffness characteristics.

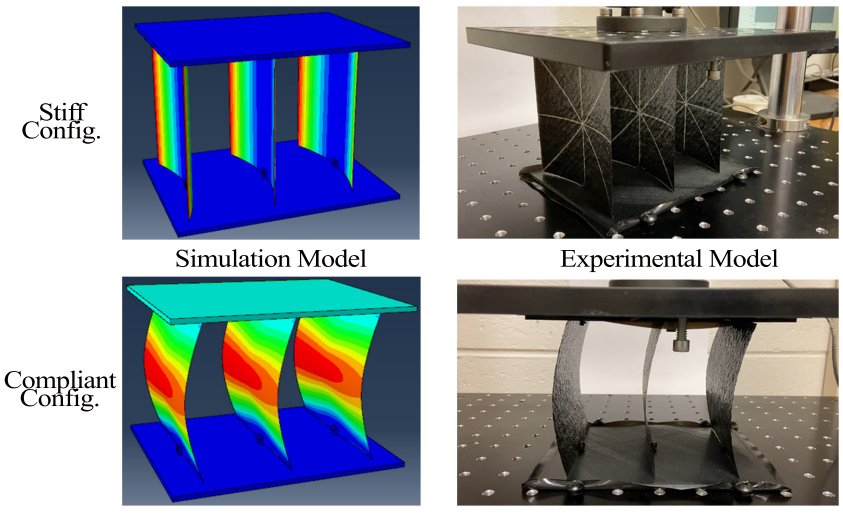

Figure 1: The stiff and compliant configurations of the stiffness switchable structure. Here, we use both finite element simulations and experimental images to demonstrate the working principle.

2.1 Design and Construction:

Figure 2 illustrates the overall design and working principle of the dual-stiffness sandwich structure. The asymmetric laminates at the core of this structure can settle into two distinct stable states corresponding to the stiff and compliant configuration. The difference in the overall structural stiffness originates from the change of these laminate's curved shapes between their two stable states.

We use asymmetric square laminates of $[0°/90°]$ fiber ply arrangement and 100mm × 100mm dimension – a classical design considered in many previous studies.[15,24] These laminates are made from Grafil TR50s carbon fibers prepregs with Newport 301 resin, and they are cured in an industrial oven at 135°C using the vacuum bagging technique. The fabrication processes are detailed in the authors' previous paper.[24] Table 1 summarizes the constitutive material properties.

To construct the switchable structure, we attach the square laminates in parallel to two end plates, which can bear the external loads and provide the necessary boundary conditions for these laminates (Figure 2). The end plates are precisely 3D-printed using black Nylon material in the Ultimaker Cura S5 printer. Figure 2(B) shows the detailed geometry of these end plates, which feature small rectangular extrusions with adequate thickness and a hole in the middle. Via bolted connection (small 2-56 sized bolts), the asymmetric laminate is carefully fixed to these small rectangular extrusions so that their upper and lower edges rest on the end plates' surface without any localized buckling near the bolted connection. We use finite element simulation to determine the appropriate size of these extrusions and the corresponding hole position for laminate-end plate connection, as detailed in the following sub-section.

2.2 Finite Element Simulation

The finite element simulation is carried out in `ABAQUS CAE2020` using the *Static General* module. We mesh the square geometry of the laminates using 3D-deformable `S4R` shell elements with a mesh size of 2.5mm. The laminate's geometry has holes at the mid-point of two opposite edges (top and bottom), connecting to the extrusions on the end plates. The end plates are modeled as rigid bodies, and the contact between the laminates' edges and the end plates' surface is defined using two properties: *Normal Behaviour* = "Hard Surface" and

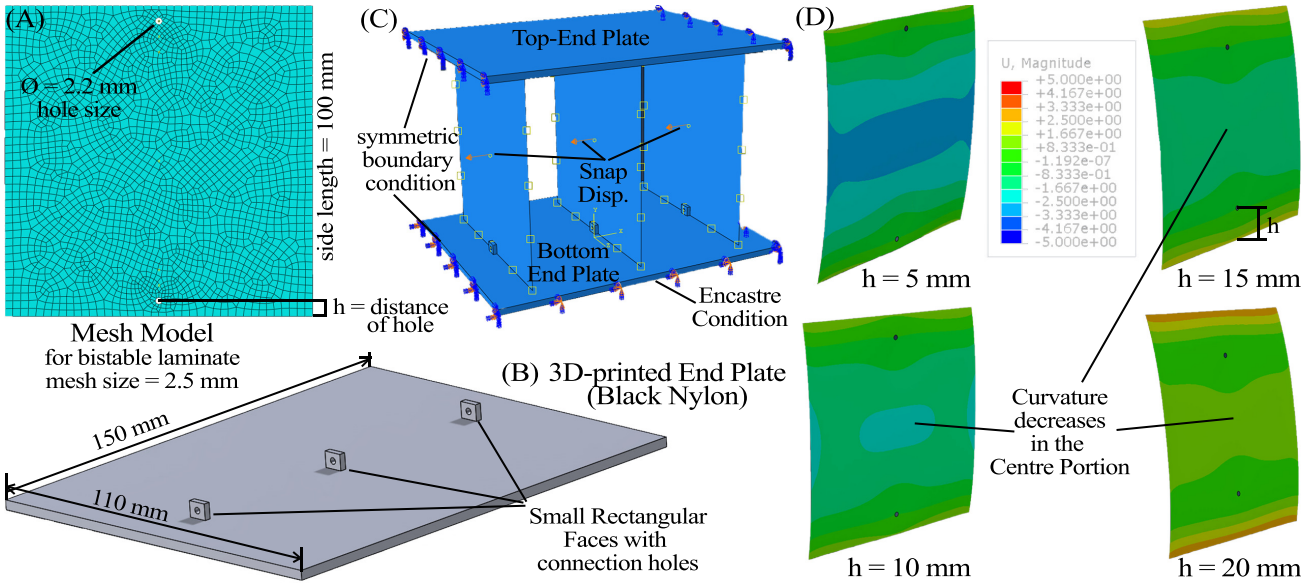

Figure 2: The overall design and construction of the dual stiffness switchable structure. (A) The mesh geometry for the bistable square laminate, showing the two holes for bolt connection with the end plats. (B) 3D-printed end plate. (C) The overall construction of the switchable structure and different boundary conditions used in the finite element simulation. (D) The influence of "h" — distance between the connecting holes and top (or bottom) edge — on the curvature of the laminate after snap-through.

Tangential Behaviour = "Frictionless," representing a perfect contact condition. The laminate and the end plates' small rectangular extrusion are bonded using the *Tie* constraint.

Finite element simulation involves three steps. The first step simulates the curing of laminates to stiff configuration. In this step, the laminates are heated to 135°C first and cooled down to room temperature at 20°C. They then stabilize to a curved stable configuration, shaped like a curved wall. The second step simulates the snap of the asymmetric laminate to the compliant configuration. At this step, we apply sufficient transverse displacement to the center points of all laminates (Figure 2(c)), snapping them to the other stable state. The third step involves "Free Damping." All the laminates are relieved of any external displacements and loads to double-check whether the sandwich structure can remain at the compliant configuration.

We find that the position of connection holes on the laminate significantly affects the structures' switching behaviors between the stiff and compliant configurations. In Figure 2(a), "h" in the mesh geometry refers to this position of connection holes. As the two holes approach the laminate's center, the asymmetric laminates become flatter at their compliant configuration. This phenomenon could be observed in figure 2(D). Here, we place the tie constraints at 5mm, 10mm, 15mm, or 20 mm away from the top or bottom laminate edges as the possible positions of the connection hole. By comparing these finite element simulations, one can conclude that the connecting hole's optimum position is 5mm for several reasons. First, the laminate retains the desired curved shape at the compliant configuration, ensuring stronger bistability and a higher variation in stiffness. Secondly, the 5mm distance from the laminate's edge is sufficient to prevent fibers damage or localized material weakening. Third, 5mm distance offers the minimum resistance to laminates' shape changes so that the structure can be switched easily between two stable states. Finally, due to manufacturing imperfection, the laminate's top and bottom edges may not be fully in contact with the end plates. This means that these connection points will transfer a significant part of the applied load to the central portion of the laminates. Hence, a larger distance between the connecting holes and laminate edges means that a smaller portion of the laminate has to bear external load, which might increase the chances of early structural failure.

2.3 Experimental Method

Based on the optimal designs obtained in the finite element analysis, we constructed a proof-of-concept prototype and measured the force-displacement curves at their stiff and compliant configurations. In these tests, we fix the lower end plate of the sandwich structure using bolts to the base plate of the ADMET eXpert 5061 universal testing machine. The upper end plate connects to the load cell (S-type with a maximum range of 25lbs or 111N) and is compressed with a fixed displacement rate of 0.5mm/sec. In this study, the snap between stiff and compliant configurations is achieved manually.

2.4 Results and Discussion

The central graph in the figure 3 summarises the responses from two configurations, and the difference between these two is characterized in terms of fitted stiffness within various loading regions. Asymmetric composite laminates act like thin walls with a curved shape in the stiff configuration. Their fiber plies, which have fibers aligned with the loading direction, take up a significant load until buckling. Hence, the response shows a stiff behavior in that the reaction force reaches approximately 111N (the maximum limit of the load cell) at a displacement less than 2.5mm. We observe two regions in the stiff force-displacement curve that show a linear trend and calculate the corresponding stiffness: The first linear region ranges from 0.65mm to 1.24mm, with a magnitude of 85N/mm. The second linear trend is observed from 1.80mm to 2.13mm of displacement, with a

Table 1: Constituent material properties of Grafil TR50s carbon fibres with Newport 301 resin carbon composite prepregs and thickness = 0.117mm. E_i and G_{ij} are the elastic modulus (unit of GPA). ν is the Poisson's ratio. α_{ij} are the thermal coefficients of expansion (unit of $^\circ C^{-1}$).

Property	Value	Property	Value	Property	Value
E_1	140	G_{12}	5	α_{11}	-2×10^{-8}
E_2	9.4	G_{13}	7.17	α_{22}	2.4×10^{-5}
ν_{12}	0.3	G_{23}	3.97	α_{33}	2.4×10^{-5}

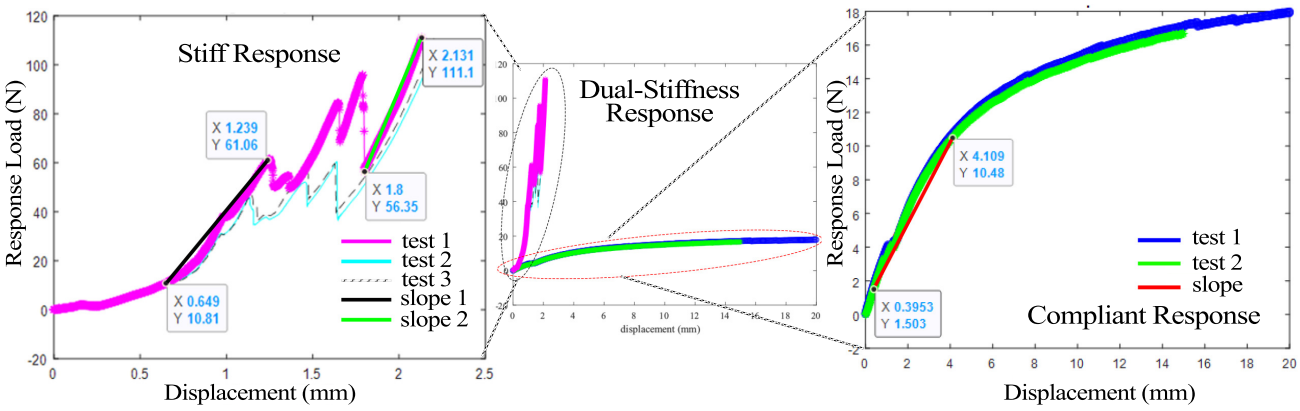

Figure 3: Dual stiffness response of the structure showing the reaction load (in N) vs displacement (in mm). The red line shows the estimated slope of the initial part of the curve and the two data points are used to estimate this slope, or stiffness.

stiffness magnitude of 165N/mm. The two linear regions in the stiff force-displacement result from manufacturing imperfections at the boundary edges of the laminate. In the first linear region, only a single laminate is in contact with the top and bottom end plates. Once this laminate buckles, the other two laminates come in contact with the end plates, providing a higher stiffness response as indicated by the second linear region. Indeed, one can see that the fitted stiffness in the second linear region is nearly two times that of the first region. Nonetheless, our future study will improve the fabrication accuracy to avoid this inconsistent buckling.

When the structure switches to the compliant configuration, the asymmetric composite laminates buckle and deform like compliant springs with much lower resistance to the external force. In this configuration, the experimentally measured reaction force is lower than 18N, even at a considerable top end plate displacement at 20mm. The stiffness for compliant configuration, calculated in the initial linear response range, is 2.4N/mm. Therefore, a high stiffness ratio transition of $\approx 70:1$ is achievable. This sandwich structure shows immense promise in lightweight systems that demand stiffness control for morphing and suggests more research to prescribe this stiffness change ratio as a function of its geometry and construction.

3. CASE STUDY 2: SWITCHABLE KRESLING ORIGAMI STRUCTURE

Kresling origami originates from the buckling and collapsing of a cylindrical shell under compression,[25] and it has found many applications in deployable structures[26,27] and robotics.[28,29] In this case study, we evolve the Kresling origami by integrating the asymmetric composite bistability with its traditional design, creating a new structure that can switch between a "foldable" configuration and a "locked" configuration.

3.1 Design and Fabrication:

The new Kresling structure consists of three main components: (1) a Kresling skin made of 3D-printed soft TPU material, (2) end plates made from stiff Nylon material (also 3D printed), and (3) triangular-shaped asymmetric laminates made from the above mentioned CFRP prepreg. The Kresling skin (Figure 4(C)) serves as the skeleton of this structure. Its flexibility allows it to fold and unfold easily, generating the creases in the traditional Kresling origami design. These skins have triangular cavities in their facets to accommodate the asymmetric laminates, as well as five holes on the top and bottom to connect to the end plates. In this case study, we select $L = R = 60\ mm$ as the side length of the regular hexagonal base, the angle $\theta = 60°$, and angle fraction $\lambda = 0.8$ (Figure 4 (A)). Each end plate is an assembly of two components: the outer plate and inner plate (Figure 4(D)); the inner plate has teeth on its periphery that slide into the holes on the outer plate, locking the relative motion between the two. Finally, asymmetric two-ply laminates are added to the triangular-shaped cavities in the Kresling skin. These laminates all have one fiber ply layer aligned in the crease direction and the other in the corresponding perpendicular direction.

To fabricate the Kresling origami, we first assemble its facets by attaching uncured laminate prepregs to the 3D printed kresling skin, then oven-cure the facet assembly using the same vacuum bagging techniques. The

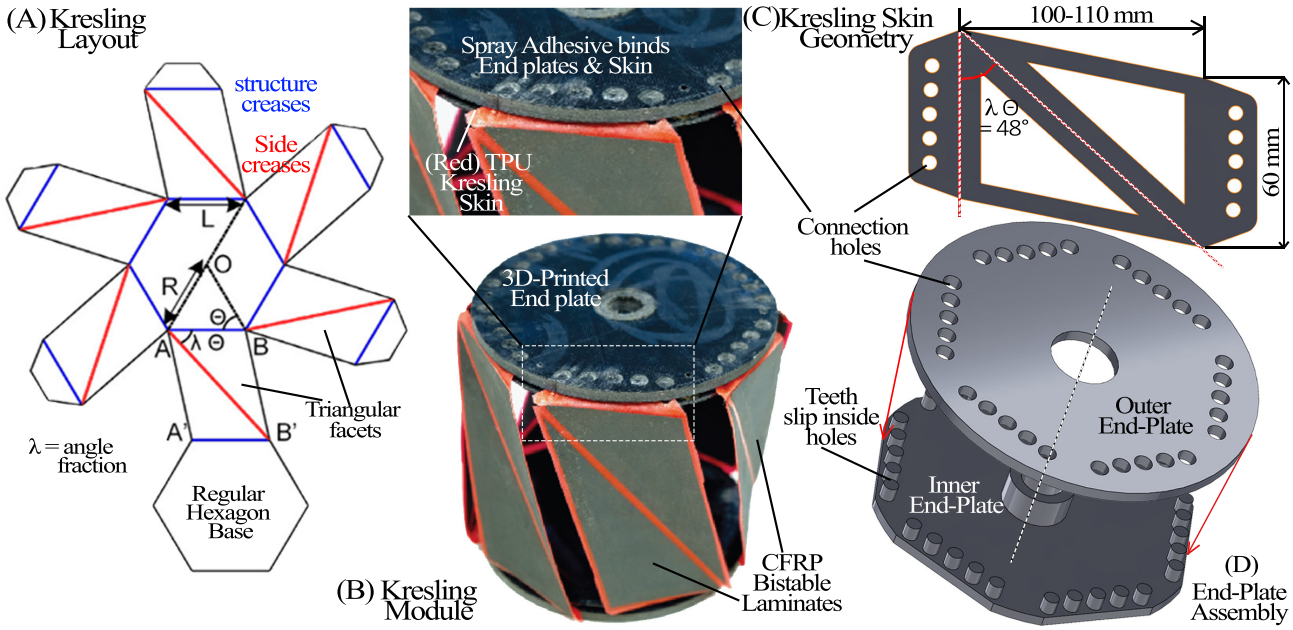

Figure 4: Switchable composite Kresling structure: Design parameters and fabrication

cured Kresling facets are installed, via the holes on the skin, in between the two components of the endplates (refer Figure 4(B), where the enlarged image show the end plate assembly and the TPU skin installed in between the plates). We ensure that the Kresling facets are buckled outwards in this assembly process. Finally, the two parts of the endplates are glued together with spray adhesive.

3.2 Testing Results and Discussion

Once assembled, the Kresling structure is evaluated for its switchable behavior between foldable and locked configurations. More specifically, the assembled Kresling can stabilize itself in either a foldable State-1 or locked State-2 as shown in Figure 5(B). At the foldable State-1, the Kresling's side facets curve inwards, and its creases carry most of the external load. As a result, we can apply only a small axial force to fold the Kresling into a collapsed configuration, where all creases are folded to their maximum. We refer to this collapsed configuration as State-0 in Figure 5(B). Such folding (and twisting) from State-1 to 0 is consistent with the kinematics of traditional Kresling origami design. Once the external force is released, the Kresling quickly unfolds itself and returns to State-1.

To measure the compression force-displacement relationship of the Kresling at foldable configuration, we use the same Universal Testing machine mentioned in Section 2.3. A custom-made, free-rotating platform is installed on the tester machine to accommodate the Kresling's twisting during folding. The green-colored loading cycle shown in Figure 5(A) shows the response in foldable configuration between State-1 and 0. The State-1 is at the leftmost point of this cycle ($\sim$ -50mm displacement), and the State-0 is at the right-most (50mm displacement). Therefore, the total stroke of the foldable Kresling is near 100mm. More importantly, besides a slight increase in reaction force near the State-0 (the slight increase in stiffness could be attributed to the folded kresling sides coming in contact at the end profile of the test and providing a small compression resistance), the foldable Kresling shows minimal resistance to external load.

In contrast to foldable State-1, the Kresling structure shows fundamentally different kinematic behaviors in the locked State-2. In this locked configuration, the side facets curve outwards, so the Kresling will not fold and collapse under compression load. Instead, the facets bend outwards so that the stiff composite laminates, rather than the soft crease materials, carry most of the external load (Figure 5(B)). We can switch the Kresling from foldable State-1 to locked State-2 by simply twisting its end plates in the opposite direction to the folding-induced twisting direction. However, the reverse twist would not switch the locked Kresling back to its foldable

State-1. This unique locked configuration and the corresponding switching behavior originate from the internal stress embedded in the asymmetric composite laminate facets.

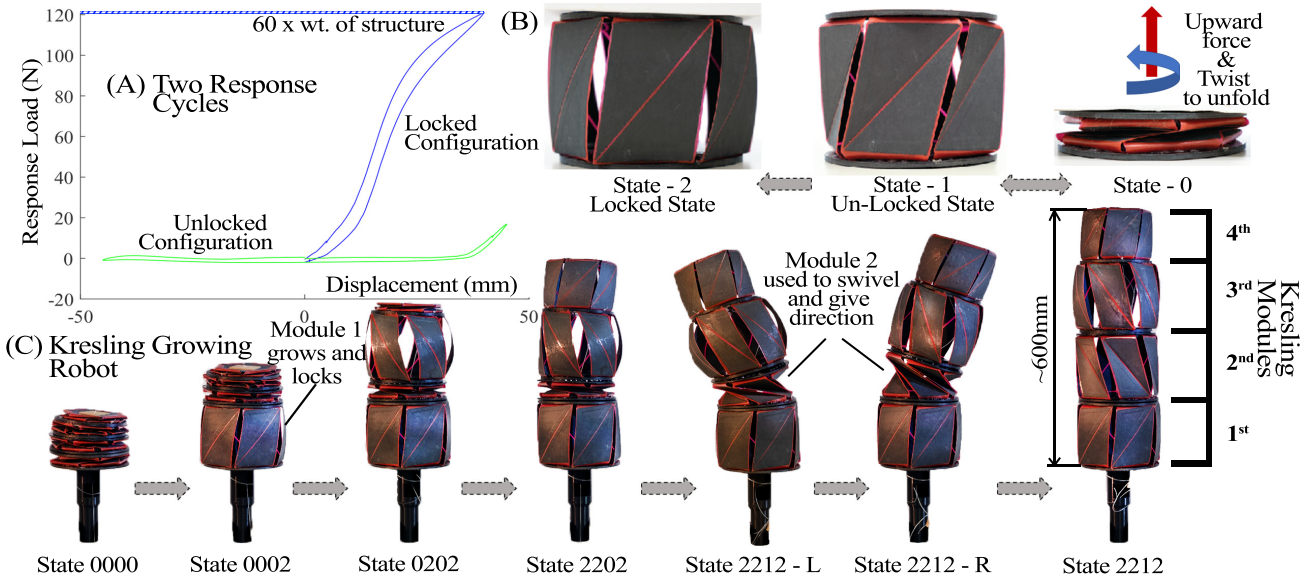

Figure 5: Switching behavior and potential applications of the composite Kresling origami. (A) Experimentally measured force-displacement curves of the Kresling in foldable (green) and locked (blue) configurations. (B) The Kresling origami at three different states – State-0 fully collapsed state, State-1 expanded but yet foldable where the kresling sides are still buckled inwards, and State-2 showing fully locked module that resists to fold. (C) A conceptual demonstration of the Kresling-based growing robotic trunk.

Moreover, the locked Kresling offers significantly higher loading bearing capacity upon compression. The blue loading cycle in Figure 5(A) shows the response at the locked configuration. The Kresling supports almost 60 times its own weight ($\approx$ 200 grams) during the compression test, with only 40mm displacement.

A promising application of the switchable Kresling structure is a "Kresling-based growing robot." The idea is to assemble various Kresling modules into a robotic trunk and mimic plant-like growth behavior by exploiting their (un)folding and locking behaviors. Figure 5(C) demonstrates a preliminary example of such a growing robot, where four Kresling modules are axially connected. We label the configurations of this robot using a simple naming scheme: If a Kresling module is at the fully-folded (or collapsed) State-0, the associated number is "0." If the module is at its unfolded (extended) State-1 without locking, the corresponding label is "1." Finally, if the module is at the fully extended and locked State-2, we label it by "2." For example, the second image in Figure 5(C) is labeled as 0002 because the first module at the base is fully extended and locked. Therefore, one can mimic the irreversible plant growth by activating the Kresling module from the fully compressed State-0 (before growth) to extended State-1 (during growth) and finally to locked State-2 (growth complete). In the fifth and sixth image in Figure 5(C), we set the second module from the base at State-1, which has some bending flexibility for robotic maneuver. It could be swiveled 360°to search the appropriate direction for the robot to grow. Here, we show two directions with respect to the viewpoint – *left* denoted as 'L' and *right* denoted as 'R'.

4. SUMMARY AND CONCLUSION

Asymmetric carbon fiber reinforced composite has shown great potential as a building block of multi-functional structural systems because of its bistability – a phenomenon that the composite can settle into two distant stable configurations. Moreover, since the asymmetric composites consist of unidirectional carbon fibers, their mechanical properties become highly directional and switchable. While the composite's behaviors under out-of-plane loading have been well studied, their response to in-plane loading remains an open question. Therefore,

we present two case studies of switchable structures by exploiting the unique *in-plane* responses of asymmetric composites.

Case study 1 elucidates that loading the asymmetric laminates in their in-plane directions could generate two significantly different stiffness responses – stiff and compliant – and the stiffness is switchable through a simple snap-through of the laminates. To illustrate the potential of such stiffness variation, we proposed a sandwich structure design consisting of three asymmetric and bistable laminates, each of which fixed to two 3D-printed end plates using bolted connections. In preliminary experiments, this structure provides a stiffness variation ratio of $\approx 70:1$, and the results suggest promising potentials for further performance improvement.

In case study 2, we propose an innovative idea of adding a locking feature to the Kresling origami design by introducing the bistable nature of asymmetric composites. Kresling traditionally shows a twisting and collapsing behavior during folding. However, one could introduce asymmetric composites to its side triangular facets. The internal stress from these composites could buckle the facet outwards, creating a locking effect that no longer allows folding. Hence, we observe a kinematic switching in the structure's morphing capability (modes). Therefore, introducing asymmetric composites to origami/kirigami could resolve the challenges of maintaining the folded shape without any external aid. Finally, we demonstrate the potential of such a folding-locking switch via a plant-inspired, growing robotic branch concept.

Overall, the results of this study open new avenues towards exploiting the in-plane response of bistable CFRPs to advance and enrich the functionalities of adaptive structural systems for many different applications.

Acknowledgement

The authors acknowledge the support from the National Science Foundation (CMMI-1760943, 1933124).

REFERENCES

[1] Daynes, S. and Weaver, P. M., "A morphing trailing edge device for a wind turbine," *Journal of Intelligent Material Systems and Structures* **23**(6), 691–701 (2012).

[2] Panesar, A. S. and Weaver, P. M., "Optimisation of blended bistable laminates for a morphing flap," *Composite Structures* **94**, 3092–3105 (oct 2012).

[3] Diaconu, C. G., Weaver, P. M., and Mattioni, F., "Concepts for morphing airfoil sections using bi-stable laminated composite structures," *Thin-Walled Structures* **46**(6), 689–701 (2008).

[4] Kuder, I. K., Fasel, U., Ermanni, P., and Arrieta, A. F., "Concurrent design of a morphing aerofoil with variable stiffness bi-stable laminates," *Smart Materials and Structures* **25**(11) (2016).

[5] Arrieta, A. F., Hagedorn, P., Erturk, A., and Inman, D. J., "A piezoelectric bistable plate for nonlinear broadband energy harvesting," *Applied Physics Letters* **97**(10), 95–98 (2010).

[6] Dano, M. L. and Hyer, M. W., "Snap-through of unsymmetric fiber-reinforced composite laminates," *International Journal of Solids and Structures* **40**(22), 5949–5972 (2000).

[7] Arrieta, A. F., Kuder, I. K., Waeber, T., and Ermanni, P., "Variable stiffness characteristics of embeddable multi-stable composites," *Composites Science and Technology* **97**, 12–18 (2014).

[8] Algmuni, A., Xi, F., and Alighanbari, H., "Design and analysis of a grid patch multi-stable composite," *Composite Structures* **246**(January), 112378 (2020).

[9] Emam, S. A. and Inman, D. J., "A Review on Bistable Composite Laminates for Morphing and Energy Harvesting," *Applied Mechanics Reviews* (2015).

[10] Fiorito, F., Sauchelli, M., Arroyo, D., Pesenti, M., Imperadori, M., Masera, G., and Ranzi, G., "Shape morphing solar shadings: A review," *Renewable and Sustainable Energy Reviews* **55**, 863–884 (2016).

[11] Ai, Q., Weaver, P. M., Barlas, T. K., Olsen, A. S., Madsen, H. A., and Andersen, T. L., "Field testing of morphing flaps on a wind turbine blade using an outdoor rotating rig," *Renewable Energy* **133**, 53–65 (2019).

[12] Dai, F., Li, H., and Du, S., "A multi-stable lattice structure and its snap-through behavior among multiple states," *Composite Structures* **97**, 56 – 63 (2013).

[13] Udani, J. P. and Arrieta, A. F., "Analytical Modeling of Multi-sectioned Bi-stable Composites: Stiffness Variability and Embeddability," *Composite Structures* **216**(November 2018), 228–239 (2019).

[14] Daynes, S. and Weaver, P. M., "Review of shape-morphing automobile structures: Concepts and outlook," *Proceedings of the Institution of Mechanical Engineers, Part D: Journal of Automobile Engineering* **227**(11), 1603–1622 (2013).

[15] Deshpande, V., Myers, O., Fadel, G., and Li, S., "Transient snap-through of a bistable composite laminate under asymmetric point load," (April), 93 (2020).

[16] Potter, K., Weaver, P., Seman, A. A., and Shah, S., "Phenomena in the bifurcation of unsymmetric composite plates," *Composites Part A: Applied Science and Manufacturing* **38**(1), 100–106 (2007).

[17] Deshpande, V., Myers, O., Fadel, G., and Li, S., "Transient deformation and curvature evolution during the snap-through of a bistable laminate under asymmetric point load," *Composites Science and Technology* **211**(November 2020), 108871 (2021).

[18] Zhang, Z., Wu, H., Ye, G., Yang, J., Kitipornchai, S., and Chai, G., "Experimental study on bistable behaviour of anti-symmetric laminated cylindrical shells in thermal environments," *Composite Structures* **144**, 24–32 (2016).

[19] Chillara, V. S., Ramanathan, A. K., and Dapino, M. J., "Self-sensing piezoelectric bistable laminates for morphing structures," *Smart Materials and Structures* **29**(8) (2020).

[20] Dano, M.-L., Jean-St-Laurent, M., and Fecteau, A., "Morphing of Bistable Composite Laminates Using Distributed Piezoelectric Actuators," *Smart Materials Research* **2012**, 1–8 (2012).

[21] Murray, D. V. and Myers, O. J., "Modeling Bistable Composite Laminates for Piezoelectric Morphing Structures," *ISRN Materials Science* **2013**, 1–12 (2013).

[22] Betts, D. N., Kim, H. A., and Bowen, C. R., "Modeling and optimization of bistable composite laminates for piezoelectric actuation," *Journal of Intelligent Material Systems and Structures* **22**(18), 2181–2191 (2011).

[23] Saberi, S., Abdollahi, A., and Inam, F., "Reliability analysis of bistable composite laminates," *AIMS Materials Science* **8**(1), 29–41 (2021).

[24] Lele, A., Deshpande, V., Myers, O., and Li, S., "Snap-through and stiffness adaptation of a multi-stable Kirigami composite module," *Composites Science and Technology* **182**(May), 107750 (2019).

[25] Hunt, G. W. and Ario, I., "Twist buckling and the foldable cylinder: an exercise in origami," *International Journal of Non-Linear Mechanics* **40**(6), 833–843 (2005).

[26] Jianguo, C., Xiaowei, D., Ya, Z., Jian, F., and Yongming, T., "Bistable Behavior of the Cylindrical Origami Structure With Kresling Pattern," *Journal of Mechanical Design* **137** (06 2015). 061406.

[27] Reid, A., Lechenault, F., Rica, S., and Adda-Bedia, M., "Geometry and design of origami bellows with tunable response," *Phys. Rev. E* **95**, 013002 (Jan 2017).

[28] Bhovad, P., Kaufmann, J., and Li, S., "Peristaltic locomotion without digital controllers: Exploiting multi-stability in origami to coordinate robotic motion," *Extreme Mechanics Letters* **32**, 100552 (2019).

[29] Novelino, L. S., Ze, Q., Wu, S., Paulino, G. H., and Zhao, R., "Untethered control of functional origami microrobots with distributed actuation," *Proceedings of the National Academy of Sciences* **117**(39), 24096–24101 (2020).